AIMETA 2017
XXIII Conference
The Italian Association of Theoretical and Applied Mechanics
Luigi Ascione, Valentino Berardi, Luciano Feo, Fernando Fraternali and Antonio Michele Tralli (eds.)
Salerno, Italy, 4–7 September 2017

NON-PRISMATIC THIN-WALLED BEAMS: CRITICAL ISSUES AND EFFECTIVE MODELING

Giuseppe Balduzzi[1], **Elio Sacco**[2], **Ferdinando Auricchio**[3], **and Josef Füssl**[1]

[1] Institute for Mechanics of Materials and Structures, TU Wien
Karlsplatz 13/202, 1040 Vienna, Austria
e-mail: Giuseppe.Balduzzi@tuwien.ac.at, Josef.Fuessl@tuwien.ac.at

[2] Department of Civil and Mechanical Engineering, University of Cassino and Southern Lazio
via di Biasio 43, 03043 Cassino, Italy
e-mail: sacco@unicas.it

[3] Department of Civil Engineering and Architecture, University of Pavia
via A. Ferrata, 27100 Pavia, Italy
e-mail: ferdinando.auricchio@unipv.it

Keywords: tapered beam, FSDT (First-order Shear Deformation Theory), cross-section stress distribution.

Abstract. *This work aims at highlighting critical issues that occurs in the modeling of mono-symmetric non-prismatic thin walled beams. In particular, even considering the simplified assumption of planar behavior, it is possible to demonstrate that the shear stress distribution within non-prismatic beams is substantially different from the one that occurs in prismatic beams. Furthermore, such a difference can not be neglected also in tapered beams with extremely smooth variation of the cross-section geometry. First, the work provides an accurate literature review, continues with the synopsis of a recently proposed enhanced strategy for the reconstruction of the stress distributions, and, finally, demonstrates its capabilities through a simple numerical example.*

1 INTRODUCTION

Shear stress distributions within homogeneous planar tapered beams are substantially different from the stress distribution within prismatic beam, as noticed since the beginning of past century [1, 2, 3]. In particular, [2] provides the stress distribution (i.e., the analytical solution of the equilibrium Partial Differential Equation (PDE)) for an infinite long wedge loaded in the apex. The analytical solution is given in a Polar coordinate system and uses trigonometric functions, nevertheless the authors specify that, for a taper angle $\alpha < 15\,\text{deg}$ and using a Cartesian coordinate system, the distributions of axial and shear stresses could be approximated with a linear and a quadratic function, respectively. If the distribution of axial stress turns out being identical to the one that can be found using stress recovery formulas used for prismatic beams, the shear stress distribution is substantially different. In fact, considering a load perpendicular to the wedge bisector (i.e., cross-sections are loaded with a shear force V and a bending moment $M = Vx$ where x denotes the distance from the apex), the shear stress has maximal value on the boundaries and vanishes on the bisector. As a consequence, the bisector fiber is unloaded whereas the boundary fibers are loaded with both the maximal horizontal stress and the maximal shear stress which magnitude, furthermore, is three times the average (in prismatic beams, conversely, the central fiber is loaded with the maximal shear stress that is 1.5 times the magnitude average) [4].

As a consequence, as noticed since the Sixty years of the past century, such a situation leads the prismatic beam models to be no longer effective for non-prismatic beams also considering small taper angles [5]. Furthermore, recent contributions have highlighted that the non trivial shear stress distribution (i) depends on all internal forces [6, 7], (ii) deeply influences the constitutive relation [8], and (iii) leads the beam stiffnesses substantially different than for prismatic beams [9]. Conversely, national and international standards (e.g., [10, 11]) provide indications for the evaluation of tapered beam buckling resistance, but do not provide any specific indication for the evaluation of the cross-section resistance, leading practitioners to suppose that prismatic beam formulas can be used also for non-prismatic beams [12]. Accordingly, most of the research focuses on enhanced aspects, like Finite Element (FE) modeling [13, 14], buckling resistance [15, 16], post-buckling behavior [17, 18], and dynamics [19], but ignores the influence of stress distribution undermining the effectiveness of any enhanced modeling approach.

To the authors' knowledge, the few attempts that aim at an enhanced recovery of cross-section stress distribution are listed in the following.

- [20] that proposed ad-hoc formula for the estimation of maximum shear-stress in non-prismatic beams. Unfortunately, in [21, 22] it is highlighted that the so far introduced formula leads to contradictory results and is not able to predict the real resistance of variable depth beams.
- [23] that proposed a simplified approach accounting for the contribution of flanges to the shear stress resistance.
- [24] that proposed an enhanced approach, but neglected flanges contribution to the vertical equilibrium.
- [8, 6] that proposed an accurate stress recovery procedure based on a suitable generalization of the Jourawsky theory [25].

[26] evaluates the effectiveness of the so far introduced methods for tapered bi-symmetric thin walled I beams, demonstrating that methods proposed in [20, 23, 24] could underestimate the

maximal shear stress up to 70 % and the Mises stress (i.e., the cross-section resistance) up to 55 %. Conversely, the stress recovery proposed in [6] results much more accurate, leading to errors exceptionally greater than 3 %. Finally, [6] also highlights that any variation of the geometry leads the shear strain to depend on all internal forces.

This paper aims at evaluating the effectiveness of the stress recovery procedure proposed in [6] for mono-symmetric thin walled beams behaving under the assumption of plane stress. The paper is structured as follows: Section 2 resumes the stress representation proposed in [6], Section 3 reports several numerical results for a T section with tapered flange and parabolic shaped web, and Section 4 discusses final remarks.

2 STRESS RECOVERY PROCEDURE

This section illustrates the main steps of the stress recovery procedure. It consists in a generalization of the stress representation proposed in [6] for multilayer non prismatic beams.

We consider the homogeneous isotropic beam depicted in Fig. 1 that is symmetric with respect to the plane $z = 0$ and behaves under the hypothesis of small displacements and plane stress state. In particular, we assume that the beam depth $b(x,y)$ is a piecewise function defined within each layer Ω_i. Finally, the material that constitutes the beam body is homogeneous, isotropic, and obeys a linear-elastic constitutive relation.

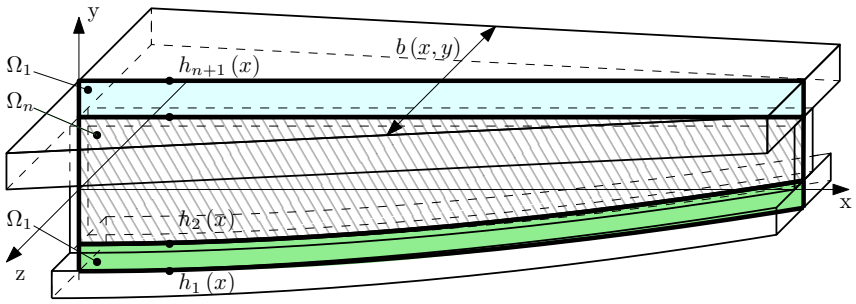

Figure 1: Beam geometry, coordinate system, dimensions and adopted notations.

We start by introducing the cross-section area $A^* : L \to \mathbb{R}$ and the first moment of area $S^* : L \to \mathbb{R}$ defined as

$$A^*(x) = \int_{h_1(x)}^{h_{n+1}(x)} b(x,y)\, dy; \quad S^*(x) = \int_{h_1(x)}^{h_{n+1}(x)} b(x,y)\, y\, dy \tag{1}$$

Consequently, the beam centerline $c : L \to \mathbb{R}$ reads

$$c(x) = \frac{S^*(x)}{A^*(x)} \tag{2}$$

Finally, we define the cross-section inertia $I^* : L \to \mathbb{R}$

$$I^*(x) = \int_{h_1(x)}^{h_{n+1}(x)} b(x,y)\,(y - c(x))^2\, dy \tag{3}$$

Assuming that the cross-section behaves as a rigid body and introducing the horizontal-stress distribution functions d_σ^H and d_σ^M defined as

$$d_\sigma^H(x,y) = \frac{1}{A^*(x)}; \quad d_\sigma^M(x,y) = \frac{1}{I^*(x)}\,(c(x) - y) \tag{4}$$

the horizontal stress distribution within the cross-section reads

$$\sigma_x(x,y) = d_\sigma^H(x,y)\,H(x) + d_\sigma^M(x,y)\,M(x) \tag{5}$$

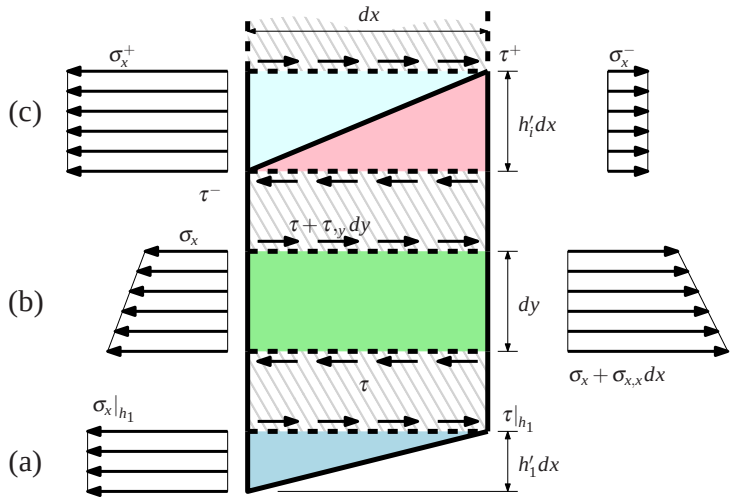

Figure 2: Equilibrium of a slice of beam of length dx: (a) equilibrium evaluated at the lower boundary, (b) equilibrium evaluated within a layer cross-section, and (c) equilibrium evaluated at an interlayer surface.

Focusing on the triangle depicted in blue in Fig. 2 (a), the horizontal equilibrium of this part of the domain can be expressed as

$$\tau|_{h_1}\,dx - \sigma_x|_{h_1}\,h_1' dx = 0 \quad \Rightarrow \quad \tau|_{h_1} = h_1'\,\sigma_x|_{h_1} \tag{6}$$

By inserting Equation (5) into Equation (6) we obtain the following expression

$$\tau(x,y)|_{h_1} = h_1'(x)\,d_\sigma^H(x,y)\big|_{h_1} H(x) + h_1'(x)\,d_\sigma^M(x,y)\big|_{h_1} M(x) \tag{7}$$

Considering the rectangle depicted in green in Fig. 2 (b), the horizontal equilibrium can be expressed as

$$-\tau dx + (\tau + \tau_{,y}\,dy)\,dx - \sigma_x dy + (\sigma_x + \sigma_{x,x} dx)\,dy = 0 \tag{8}$$

Few simplifications and integration with respect to both the y and z variables lead to

$$b(x,y)\,\tau(x,y) = -\int b(x,y)\,\sigma_{x,x}(x,y)\,dy \tag{9}$$

Inserting the horizontal stresses definition (5) into Equation (9) yields the following expression

$$\begin{aligned}\tau(x,y) = -\frac{1}{b(x,y)}\Bigg(&\int b(x,y)\,d_\sigma^H{}_{,x}(x,y)\,H(x)\,dy + \int b(x,y)\,d_\sigma^M{}_{,x}(x,y)\,M(x)\,dy \\ &+ \int b(x,y)\,d_\sigma^M(x,y)\,V(x)\,dy + C\Bigg)\end{aligned} \tag{10}$$

where the constant C results from the boundary and inter-layer equilibrium.

Finally, considering the i interlayer surface depicted in Fig. 2 (c) the horizontal equilibrium between the two different layers can be read as

$$-(b\tau)^-\,dx + (b\tau)^+\,dx - (b\sigma_x)^+\,h_i' dx + (b\sigma_x)^-\,h_i' dx = 0 \quad \Rightarrow \quad [\![b\tau]\!] = h_i' [\![b]\!] \sigma_x \tag{11}$$

By inserting the horizontal stresses definition (5) into Equation (11) the following expression is obtained

$$[\![b(x,y)\,\tau(x,y)]\!] = h_i'(x)\,[\![b(x,y)]\!]d_\sigma^H(x,y)\,H(x) + h_i'(x)\,[\![b(x,y)]\!]d_\sigma^M(x,y)\,M(x) \tag{12}$$

Aiming at providing an expression of shear stress distribution similar to the one introduced for horizontal stress (5), we collect all the terms of Equations (7), (10), and (12) that depend on $H(x)$, $M(x)$, and $V(x)$, respectively. After some numerical calculation, the shear stress distribution can be defined as follows

$$\tau(x,y) = d_\tau^H(x,y)\,H(x) + d_\tau^M(x,y)\,M(x) + d_\tau^V(y)\,V(x) \tag{13}$$

3 NUMERICAL EXAMPLE

Let us consider the non-prismatic beam schematically represented in Figure 3. In greater

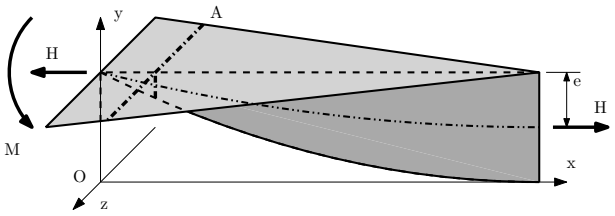

Figure 3: Thin-walled T shaped beam with tapered flange and web.

detail, $l = 5000\,\text{mm}$ and the vectors defining the cross-section geometry are

$$\begin{aligned} \boldsymbol{h}(x) &= \left[500 - 0.2x + 0.00002x^2,\, 500,\, 510\right]\,[\text{mm}] \\ \boldsymbol{b}(x) &= [10,\, 500 - 0.098x]\,[\text{mm}] \end{aligned} \tag{14}$$

Two opposite horizontal forces $H = 10\,\text{N}$ are applied in the centroids of final cross-sections and a counterclockwise bending moment $M = H * e = 10 * 250 = 2500\,\text{Nmm}$ is applied in the initial cross-section. As a consequence, the axial distribution of internal forces is

$$H(x) = 10\,[\text{N}]; \quad M(x) = 10\,(c(x) - 255)\,[\text{Nmm}] \tag{15}$$

Finally, we consider the stress recovery for the cross-section A located at $x = 1000\,\text{mm}$ and highlighted in Figure 3.

To obtain a reference solution we used a 3D FE overkill model developed using the commercial software ABAQUS [27], where we adopted a sweep mesh of wedge elements for both flange and web. Specifically, we set the wedge thickness to 1.25 mm and the characteristic dimension of wedge basis to 5 mm. Globally, 1041164 elements constituted the 3D FE model. Furthermore, we exploited the symmetry of the problem geometry with respect to the plane $z = 0$ modeling only the half of the beam body and assuming that displacements along z direction vanish for $z = 0$. Suitable displacement constraints have been imposed in order to avoid rigid body motion. Finally, we assumed that, at the beam ends, axial forces are uniformly distributed over the whole cross-section and the bending moment results from a linear stress distribution over the flange depth. In order to perform a fair comparison, in post-processing we compute the mean value of all the quantities of interest with respect to the z variable.

Figure 4 depicts the distribution of horizontal stresses σ_x in the cross-sections $x = 1000$. It

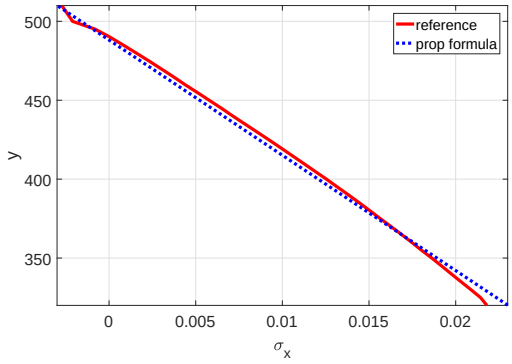

Figure 4: Axial-stress cross-section distributions

is possible to appreciate small differences between the results of the proposed formula and the reference solution. In greater detail, later-mentioned non-linearities which can be considered by the FE approach lead the proposed formula to overestimate the maximal stress on the lower boundary of the web up to 6%.

The source of the error is the fact that the proposed stress recovery strategy is based on a model that is not able to take into account higher order effects, like warping that, conversely, have a detectable influence for the considered example and are effectively caught by the 3D FE. Finally, a further error source could be the presence of boundary effect that, once more, are neglected by the model behind the proposed recovery strategy but are tackled by the 3D FE.

Figure 5 depicts the distribution of shear stresses τ in the cross-sections $x = 1000$. In general,

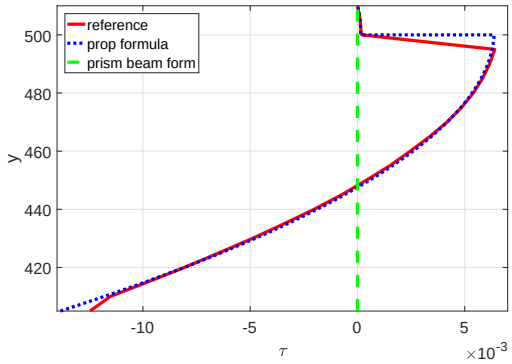

Figure 5: Shear-stress cross-section distributions

the proposed recovery strategy provides a good estimation of the shear stress distribution. Only near the bottom of the web it is possible to detect more significant errors, up to 10%. Once more, the reason of the discrepancy of the proposed recovery strategy results and the 3D FE are mainly the presence of significant higher order effects. Conversely, since the vertical internal force $V(x)$ vanishes, the prismatic-beam formula estimates vanishing shear stresses, clearly contradicting the reference solution.

4 FINAL REMARKS

Novel strategy for the recovery of stress distribution within non-prismatic mono-symmetric thin-walled planar beams has been proposed and validated trough a simple numerical example,

demonstrating that any variation of the cross section geometry induces significant effects on the distribution of shear stresses. In particular, the comparison with highly refined 3D FE solutions reveals that the proposed strategy is generally accurate, with errors usually smaller than 10% whereas the prismatic-beam formula for the shear stress estimation turns out to be unreliable since it does not allow to handle non-negligible shear stresses induced by the variation of cross-section geometry.

Since the proposed approach is based on a first-order beam model, the proposed formulas provide coarse estimations when boundary or higher order effects like warping occur. As a consequence, more refined models (e.g., 3D or shell FE, higher-order beams) are required for these situations, as recommended also for prismatic beams.

Further development of this work will include the generalization of the proposed procedure to spatial non-prismatic beams and the development of higher order beam models.

5 ACKNOWLEDGMENTS

This work was funded by the Austrian Science Found (FWF) trough the Project # M 2009-N32.

References

[1] P. Cicala. Sulle travi di altezza variabile. *Atti della Reale Accademia delle Scienze di Torino*, 74:392–402, 1939.

[2] S. Timoshenko and J. N. Goodier. *Theory of Elasticity*. McGraw-Hill, 1951.

[3] O. T. Bruhns. *Advanced Mechanics of Solids*. Springer, 2003.

[4] N.S. Trahair and P. Ansourian. In-plane behaviour of web-tapered beams. *Engineering Structures*, 108:47–52, 2016.

[5] B. A. Boley. On the accuracy of the Bernoulli-Euler theory for beams of variable section. *Journal of Applied Mechanics*, 30:374–378, 1963.

[6] G. Balduzzi, M. Aminbaghai, F. Auricchio, and J. Füssl. Planar Timoshenko-like model for multilayer non-prismatic beams. *International Journal of Mechanics and Materials in Design*. 2017. doi: 10.1007/s10999-016-9360-3.

[7] G. Balduzzi, M. Aminbaghai, and J. Füssl. Linear response of a planar FGM beam with non-linear variation of the mechanical properties. *8th Conference on Smart Structures and Materials SMART 2017*,1285–1294, 2017.

[8] G. Balduzzi, M. Aminbaghai, E. Sacco, J. Füssl, J. Eberhardsteiner, and F. Auricchio. Non-prismatic beams: a simple and effective Timoshenko-like model. *International Journal of Solids and Structures*, 90:236–250, 2016.

[9] V. Mercuri, G. Balduzzi, D. Asprone, and F. Auricchio. 2D non-prismatic beam model for stiffness matrix evaluation. In *Proceedings of the Word Conference on Timber Engineering*, 2016.

[10] Design of steel structures - Part 1-1: general rules and rules for buildings, 2005.

[11] Design of composite steel and concrete structures Part 1-1: general rules and rules for buildings, 2004.

[12] L.R. S. Marques. *Tapered steel members: flexural and lateral torsional buckling*. PhD thesis, ISISE, Departamento de Engenharia Civil Universidade de Coimbra, 2012.

[13] G. Li and J. Li. A tapered Timoshenko-Euler beam element for analysis of steel portal frames. *Journal of Constructional Steel Research*, 58:1531–1544, 2002.

[14] H. Valipour and M. Bradford. A new shape function for tapered three-dimensional beams with flexible connections. *Journal of Constructional Steel Research*, 70:43–50, 2012.

[15] A. Andrade and D. Camotim. Lateraltorsional buckling of singly symmetric tapered beams: Theory and applications. *Journal of engineering mechanics*, 131(6):586–597, 2005.

[16] A. Andrade, D. Camotim, and P. B. Dinis. Lateral-torsional buckling of singly symmetric web-tapered thin-walled i-beams: 1D model vs. shell FEA. *Computers and Structures*, 85 (17):1343–1359, 2007.

[17] S.W. Liu, R. Bai, and S.L. Chan. Second-order analysis of non-prismatic steel members by tapered beam–column elements. In *Structures*, volume 6, pages 108–118. Elsevier, 2016.

[18] C. G. Chiorean and I. V. Marchis. A second-order flexibility-based model for steel frames of tapered members. *Journal of Constructional Steel Research*, 132:43–71, 2017.

[19] S.S. Rao and R.S. Gupta. Finite element vibration analysis of rotating Timoshenko beams. *Journal of Sound and Vibration*, 242(1):103 – 124, 2001.

[20] F. Bleich. *Stahlhochbauten*, chapter 16, pages 80–85. Verlag von Julius Springer, 1932.

[21] A. Paglietti and G. Carta. La favola del taglio efficace nella teoria delle travi di altezza variabile. In *AIMETA*, 2007.

[22] A. Paglietti and G. Carta. Remarks on the current theory of shear strength of variable depth beams. *The open civil engineering journal*, 3:28–33, 2009.

[23] O. W. Blodgett. *Design of welded structures*, chapter 4.4, pages 1–8. the James F. Lincon arc welding foundation, 1966.

[24] L. Vu-Quoc and P. Léger. Efficient evaluation of the flexibility of tapered I-beams accounting for shear deformations. *International journal for numerical methods in engineering*, 33(3):553–566, 1992.

[25] D.J. Jourawski Sur le résistance dun corps prismatique et dune piece composée en bois ou on tôle de fer à une force perpendiculaire à leur longeur. *Annales des Ponts et Chaussées*, volume 12, pages 328–351, 1856.

[26] G. Balduzzi, G. Hochreiner, and J. Füssl. Stress recovery from one dimensional models for tapered bi-symmretric thin-walled I beams: deficiencies in modern engineering tools and procedures. *Thin-walled structures*, accepted, 2017.

[27] *ABAQUS User's and theory manuals - Release 6.11*. Simulia, Providence, RI, USA., 2011.